

Automatic calibration of a flood forecasting system for the Odra River

K.-P. Johnsen, J. Pestel, H. Messal and H.-T. Mengelkamp
GKSS Research Center, D-21502 Geesthacht, Germany, (johnsen@gkss.de)

Introduction

High resolution precipitation forecasts and hydrological forecasts with high accuracy are required for accurate flood forecasts. Here the calibration of the new **WRF/SEROS model system** is described. It is based on the combination of the non-hydrostatic meso-scale model WRF and the hydrological model and routing scheme SEROS. The meso-scale model WRF has been set up to downscale meteorological variables from the NCEP (National Center for Environmental Prediction) re-analysis data set with a horizontal resolution of $250 \times 250 \text{ km}^2$ to a resolution of $4.5 \times 4.5 \text{ km}^2$ for the simulation of the Odra watershed. The land use input data are taken from the CORINE data set, the orographic data are taken from the GTOPO data base of the USGS (United States Geological Survey). The downscaled precipitation fields were compared to observations. The SEROS system contains many parameters. To calibrate these parameters the shuffled complex evolution algorithm SCE-UA of the University of Arizona (Duan et al., 1993) is applied for each sub-catchment. Here we describe the set-up of the WRF model, the land surface model and the routing scheme.

2. Set up of the WRF model and coupling to SEROS

The non-hydrostatic numerical Weather Research and Forecast (WRF) Modeling System Version 2 is applied to estimate the precipitation fields over the Odra catchment between May and September 2002. Two-way nesting with three nesting levels with grid sizes of 70.4 km, 17.6 km and 4.5 km was used to downscale the meteorological variables. The time step was chosen to 30 s. Currently the Kessler microphysics scheme is used to produce the rain. For the planetary boundary layer the Yonsei University scheme, a scheme with an explicit entrainment layer and a parabolic K profile in the unstable mixed layer, is applied. To describe the cumulus parameterization the Grell-Devenyi ensemble scheme is used. The long-wave radiation is calculated with the Rapid Radiative Transfer Model (RRTM) which uses look-up tables for efficiency reasons. It accounts for multiple bands, trace gases, and microphysics species. For the shortwave radiation the Dudhia scheme is applied, a simple downward integration allowing efficiently for clouds and clear-sky absorption and scattering. For the land surface modeling within the WRF model set-up a 5-layer thermal diffusion scheme is used. All schemes are applied at all three nesting levels.

Currently a one-way coupling to the land-surface and routing scheme SEROS is realized. SEROS was forced with data of WRF every three hours. As forcing

data from the atmospheric model the precipitation since the last data record, the air temperature in the height of 2 m, the wind speed at 10 m above ground, the air pressure, the relative humidity in the height of 2 m and the short- and long-wave radiation are applied.

Mean Precipitation over the Odra River

Figures 1 and 2 show the mean precipitation over the whole Odra catchment calculated from 387 precipitation stations and compared with WRF with the nesting levels 1 and 3 (i.e. 70.4 and 4.4 km grid size).

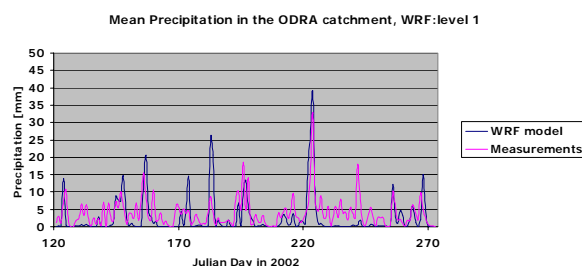


Figure 1: Mean precipitation in the Odra catchment, WRF nesting level 1.

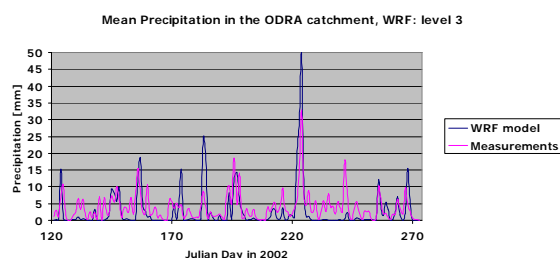


Figure 2: Mean precipitation in the Odra catchment, WRF nesting level 3.

3. The hydrological model SEROS

The hydrological model SEROS combines the one-dimensional vertical land surface scheme SEWAB (Surface Energy and Water Balance, Mengelkamp et al, 1999) and the horizontal routing scheme (Lohmann et al., 1996).

The land-surface scheme SEWAB

The one-dimensional (vertical) land surface model SEWAB is designed to be coupled to atmospheric models or be run offline with forcing data. It calculates the vertical water and energy fluxes between the land surface and the atmosphere and

within the soil column for a land surface grid cell. A land surface grid cell typically has horizontal dimensions of 1 to 100 km.

In SEWAB, both water and energy balance equations are solved at the land surface interface. The surface energy balance equation describes the equilibrium of net irradiance, latent heat flux, sensible heat flux and soil heat flux (and in case of snow, the energy available for melting). Precipitation is partitioned into runoff, evapotranspiration and change of snow pack and soil moisture storage. The evapotranspiration is calculated separately for bare soil and vegetated parts of the land surface grid cell.

The soil column (Figure 3) is divided into a variable number of model layers. Within the soil column, temperature diffusion (with a term for soil freezing) and the Richards equation are solved. The Richards equation is modified to allow for root water uptake and soil freezing. The temperature of the first model layer is solved from the surface energy balance. The lower boundary temperature is prescribed by a time series representing the annual cycle. Leaf drip, precipitation on bare soil, evaporation from bare soil and the soil moisture are accounted for.

As a one-dimensional model, SEWAB represents a land-surface grid cell of an atmospheric circulation model with dimensions ranging from 1 to more than 10000 km². Runoff from the grid cell soil column is subject to transformation and translation processes before the water reaches the river as streamflow. Runoff may occur from saturated patches inside the grid cell before saturation of the whole soil column or even may be delayed through ponding at the surface. These processes are described by the variable infiltration capacity approach for surface runoff and the concept of linear reservoirs for subsurface runoff and groundwater flow (Mengelkamp et al., 2001).

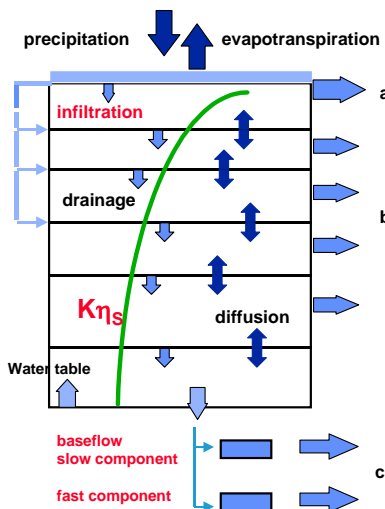


Figure 3: Sketch of the hydrological processes in SEWAB. a, b and c represent surface runoff, subsurface runoff and baseflow, respectively

The variable infiltration capacity (VIC) approach indirectly accounts for the impact that topography and soil distribution have on surface infiltration (Wood et al., 1992). This concept does not necessarily need topographic data, the parameters can be calibrated to the catchment. However, within hilly and mountainous catchments the topography determines the distribution of soil type, soil depth and water table. I.e. when calibrating the parameters for the VIC approach the indirect effect of topography on the hydrological behavior is represented.

Linear reservoirs are added to the soil column to describe subsurface runoff and baseflow (Figure 3). Subsurface runoff generation follows the ARNO model conceptualization (Dümenil and Todini, 1992). Between field capacity and saturation the outflow of any soil layer is proportional to the current soil water content in that layer and controlled by the respective time constant which is subject to calibration.

The outflow from two linear groundwater storages for the slow and fast component represents the runoff baseflow component. The storages are filled by Darcian flow from the lowest soil layer. Individual time constants for the fast and slow component are determined empirically. This concept of storages allows a subtle adjustment of surface runoff, subsurface runoff and baseflow. However, the large number of calibration parameters (time constants and storage heights) makes the calibration procedure a tedious task.

The routing scheme

The routing scheme describes the time which the runoff needs to reach the outlet of a grid box and the water transport in the river network. The river network is constructed from digital terrain data. It is assumed that water flows uni-directionally from grid box to grid box with eight possible directions through each side and all corners of the grid box. The time delay for the in-box transport of the locally generated runoff is represented by an impulse response function of the unit hydrograph (Figure 4, red curve).

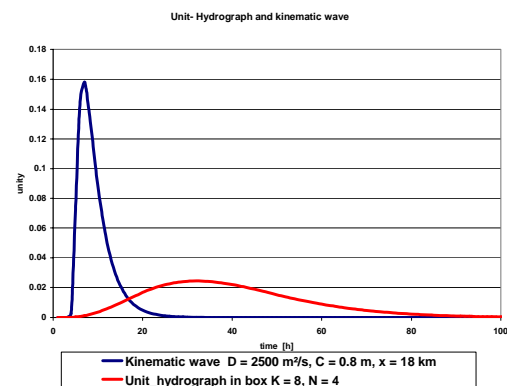


Figure 4: Unit-Hydrograph and kinematic wave.

The transport in the river system is described by an impulse response function as the solution of the linearized St. Venant equation. The scheme was originally developed by Lohmann et al. (1996). Based on the theory of a cascade of linear reservoirs the gamma probability distribution function represents the impulse response function of the unit hydrograph UH_G . The cell discharge only from cell G is

$$Q_G(t) = \int_0^t UH_G(\tau) \cdot P_{eff}(t - \tau) d\tau \quad (1.1)$$

with

$$UH_G(\tau) = \frac{1}{k(n-1)!} \left(\frac{\tau}{k}\right)^{n-1} \cdot \exp\left(-\frac{\tau}{k}\right) \quad (1.2)$$

P_{eff} effective precipitation, here sum of fast flow and baseflow
 n number of linear storages.
 k retention of storage

The storage constant k is the same for all n reservoirs. t represents the time. The parameters k and n are subject to calibration. The impulse response function at any location and time for the river routing is UH_R . The discharge of the river network (kinematic wave, Figure 4) is:

$$Q_R(G, t) = \sum_{all B} \int_0^t Q_{B,i}(t - \tau) \cdot UH_R(x_{GB_i}, \tau) d\tau \quad (1.3)$$

with

$$UH_R(x, \tau) = \frac{x}{2\tau\sqrt{\pi D \tau}} \cdot \exp\left(-\frac{(x - C\tau)^2}{4D\tau}\right) \quad (1.4)$$

here are

x_{GB_i} river length between boxes B_i and G
 C celerity (or velocity)
 D diffusivity
 $Q_{B,i}(t)$ discharge from inflow cell B_i , $\max(i)=7$.

The distance x is the natural length of the river in a grid box. D is the diffusion coefficient which can be considered as a calibration parameter. In each study it is assigned a constant value. The wave velocity C is deduced from observed streamflow data. The streamflow in the river channel at any location and time is described in equation (1.3).

The routing process is simulated in the following way: Inside each grid box runoff is generated by the land-surface scheme. This is transformed through the impulse response function UH_G into box outflow Q_G (Figure 5 left). There are also (up to 7) upstream inflows into the box in the river channel $Q_{B,i}$ (Figure 5 right). These parts of the flow are transformed by the river impulse response function UH_R to box outflow Q_R (equation 1.3.). The sum of Q_G and Q_R is the total outflow from the grid box G and represents the river inflow to the next downstream box.

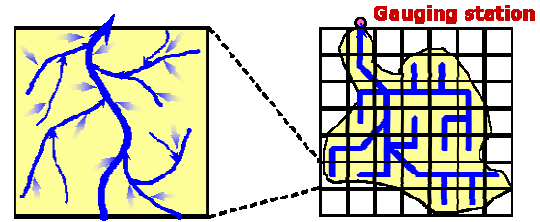


Figure 5: Horizontal water transport –grid scheme

Data, set up and calibration of the WRF/SEROS system

The routing network and sub-catchments of each gauging station are determined from a digital elevation model. The land-use type is deduced from the CORINE data set and the soil type from a polish soil type map.

Forcing data from 50 synoptic stations (6 hourly data) and 666 precipitation stations (daily data) are interpolated onto the model grid and used as forcing data. Daily discharges of 29 gauging stations and of 11 reservoirs in the mountainous region are used for calibration and verification. The calibration period was 1992 to 1994, the verification period 1995 to 1999.

The rainfall-runoff (SEWAB) and the horizontal routing scheme are based on conceptual representations of the physical processes. Conceptual representations are controlled by physical parameters that describe measurable properties of the watershed and non measurable process parameters. Despite the detailed information for vegetation cover and soil type the respective parameters cannot be exactly defined for a single grid nor a sub-catchment. These include parameters of the evapotranspiration parameterization, runoff generation, initial soil water content and the water transport in the channel system. Some parameters can be deduced from watershed properties (i.e. the length of the river inside a grid box, the partition of major vegetation types from the CORINE data set). The interception reservoir or the stomata resistance of the vegetation, the retention period of the water inside a grid box or the partition in surface and subsurface runoff can not be known a priori. These parameters are among the ones which are subject to calibration. The choice of parameters (Table I) conforms to the necessity to include the significant processes but to minimize the number of parameters.

Table I: Calibration parameter and their lower and upper limit

notation	units	description	lower	upper
BI	[-]	VIC-Parameter for surface runoff	0.001	1.00
CBAS-L3	[-]	exponent for subsurface runoff, 3 rd soil layer	1.00	3.00
T1/2-L3	[d]	time constant 3 rd soil layer	50	1000
WS-L3	[-]	fraction to baseflow from 3 rd soil layer	0.40	0.99
DM-L3	[mm/s]	maximum runoff from 3 rd soil layer	0.001	0.500
CBAS	[-]	exponent for baseflow 6 th soil layer	1.00	3.00
T1/2	[d]	time constant for baseflow 6 th soil layer	50	1000
WS	[-]	fraction to baseflow from 6 th soil layer	0.40	0.99
DM	[mm/s]	maximum runoff from 6 th soil layer	0.001	0.500
rsFactor	[-]	correction for minimum stomata res.	0.50	2.50
iniGW	[m]	initial baseflow storage	1.50	4.0
n	[-]	number of storages for unit hydrograph	1.0	4.0
k	[h]	retention period	1.0	24.0
diff	[m ² /s]	Rate of diffusion x 1000	0.8	8.0
velo	[m/s]	velocity of kinematic wave	0.2	3.0

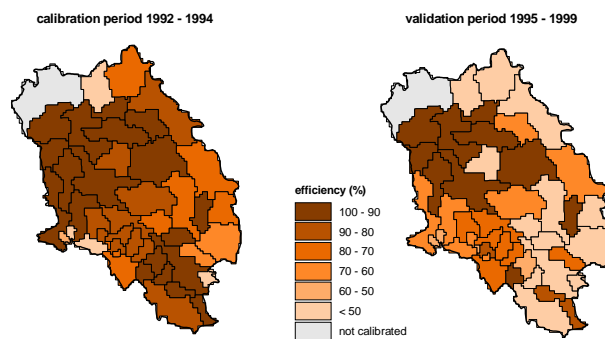


Figure 6: Nash-Sutcliffe efficiencies for the Odra watershed and the SEROS system – calibration period (left) and validation period (right).

During the calibration period 1992 to 1994 more than 80 % of the sub-catchments show an Nash-Sutcliffe efficiency over 65 %, more than 40 % of the sub-catchments reach efficiencies over 90 %. The efficiencies for the validation period 1995 to 1999 are lower (as expected) in particular in the eastern part of the Odra watershed. An explanation might be that the spatial density of precipitation stations is lowest in the eastern part and that subsurface water transports in these flat areas and some smaller reservoirs are not adequately accounted for in the model. Additionally, the validation period includes the extreme flooding event of 1997 which in some smaller sub-catchments might not be represented properly.

As one example, Figure 7 shows a comparison of the measured and modelled discharges of the sub-catchment Scinawa for the period May to September 2002. Scinawa is with 29583.8 km² one of the larger sub-catchments of the Odra river. Here SEROS was forced with WRF-precipitation data of nesting level 3. Similar results were obtained for most of the sub-catchments of the Odra river.

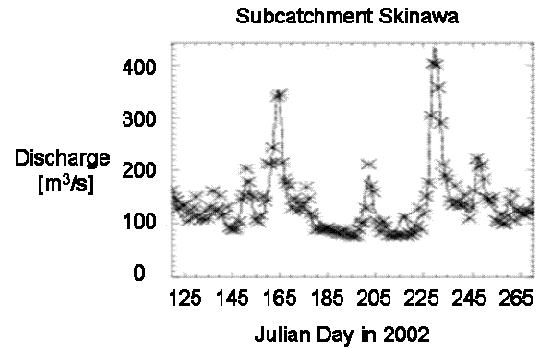


Figure 7: Comparison of the measured (asterisks) and modelled discharges (line) of the sub-catchment Scinawa of the Odra river for the period May to September 2002.

4. Conclusions

The hydrological model SEROS is coupled to the atmospheric model WRF. SEROS consists of a grid based rainfall-runoff scheme with advanced features for runoff generation and a horizontal routing scheme. The results are in reasonable agreement between observed and simulated streamflow during the validation and calibration period, the latter including the 1997 extreme flooding event. First results for the coupling of WRF and SEROS suggest that the quality of the precipitation forecast of WRF is well enough for modelling the discharge of most of the sub-catchments of the Odra river.

References

- Duan, Q., Gupta V.K., & Sorooshian S., Shuffled complex evolution approach for effective and efficient global minimization, *J. Optimization Theory and Applications*, 76, 3, 501-521, 1993.
- Dümenil, L., & Todini, E., A rainfall-runoff scheme for use in the Hamburg climate model. *Advances in theoretical hydrology, A tribute to James Dooge*. J. P. O'Kane, Ed., European Geophys. Soc. Series on Hydrological Sciences 1, Elsevier, 129-157, 1992.
- Lohmann, D., Nolte-Holube, R. & Raschke, E., A large scale horizontal routing model to be coupled to land surface parameterization schemes. *Tellus* **48A**, 5, 708-721, 1996.
- Mengelkamp, H.-T., Warrach, K., & Raschke, E., SEWAB: a parameterization of the surface energy and water balance for atmospheric and hydrologic models. *Adv. Water Res.*, **23**, 2, 165-175, 1999.
- Mengelkamp, H.-T., Warrach, K., Ruhe, C. & Raschke, E., Simulation of runoff and streamflow on local and regional scales. *Meteorol. Atmos. Phys.*, **76**, 107-117, 2001.